Comparing energy calculations: Hydraulic fracturing and microseismic monitoring

Neda Boroumand, University of Calgary, Calgary, Alberta, Canada
nborouma@ucalgary.ca
and
Dr. Dave W. Eaton, University of Calgary

GeoConvention 2012:Vision

Summary

In this paper we compare the input and output energy during a hydraulic fracture treatment to evaluate microseismic efficiency – the fraction of total input energy that is radiated as high-frequency seismic waves. We use three approaches to compute energy. "Injection energy" is the total energy input into the system, which can be accurately quantified using the product of treatment pressure, injection rate and duration. "Fracture energy" is an estimate of the work done during the deformation process. This parameter has considerably greater uncertainty and is computed using the product of the in situ treatment pressure, total effective area of the fracture surface (estimated using the microseismic event distribution) and the effective opening width of the fractures (based on an educated guess). Finally, "radiated seismic energy" is computed by summing the energy for all recorded high-frequency microseisms, after converting the reported moment magnitudes into energy based on scaling relations developed in earthquake seismology. This estimate is highly uncertain for various reasons, including epistemic uncertainty, which reflects lack of knowledge, and aleatory uncertainty, which reflects uncertainty that is inherent to the observations. Epistemic uncertainty stems primarily from the extent of extrapolation required for use of moment-energy relations, which are calibrated for large earthquakes and here are applied to events that are more than 10 orders of magnitude smaller. Aleatory uncertainty is related to noise, missing data and amplitude uncertainty due to radiation patterns. We attempted to correct the seismic energy for missing data by estimating the Gutenberg-Richter b value to estimate the contribution for all events greater than magnitude -3 up to the maximum recorded magnitude. To our knowledge, such a correction has not been previously attempted, but it is very significant for determining the seismic energy. Injection, fracture and radiated seismic energy were calculated for 10 stimulated stages. Fracture energy was found to be 12-41% of total injected energy, whereas the ratio of radiated energy to fracture energy ratio was consistently less than 1% for all stages. A current viewpoint is that the fracture energy typically represents 20-80% of the total injection energy, and that the shear mechanisms are only a small part of the total fracturing process (N. Warpinski, pers. comm., 2011). This viewpoint is adopted here as a working hypothesis. Our results confirm previous studies and show that the radiated high-frequency seismic energy constitutes a small fraction of the total energy in the system.

Theory and/or Method

Data from four different wells in an unconventional shale gas play that were hydraulically fractured are considered in this study. Microseismic maps for 10 stages were produced and used to estimate the fracture area and total high-frequency seismic energy. The following sections describe the energy calculations and the parameters extracted from each stage in order to determine these values.

Injection energy

First, the injection energy was calculated in order to define the total input energy available to perform the hydraulic fracture. Since the pumping data at the surface is readily available, the total input energy can be calculated by using the following equation:

$$E_I = \int_{t_1}^{t_2} P\,Q\,dt \quad , \tag{1}$$

where t1 and t2 are the start and end times of the treatment, P(t) is the surface treatment pressure and Q(t) is the injection rate. The injection energy can also be approximated by:

$$E_I \approx \langle P(t) \rangle \langle Q(t) \rangle \Delta t \quad , \tag{2}$$

where ⟨x⟩ denotes the average value of x and Δt is the total duration of the fracture stage. We have found in comparing the calculations using equations (1) and (2) with real data that there is only a small difference (~ 2%). For simplicity, for the rest of this paper equation 2 will be used.

Fracture Energy

Next, fracture energy was calculated to determine the useful work available to create a fracture. The following equation was used to determine the amount of energy required to generate a tensile fracture (crack opening):

$$E_F = F \times d = \langle P_d \rangle A_F\, w \quad , \tag{3}$$

where Pd is the downhole pressure (provided by the pumping company), AF is the estimated area of the fracture and w is the fracture opening width. The area of the fracture/crack was determined by measuring the total length of the microseismic map and the total height.

Fracture width needs to be large enough to accept and transport proppant. Since wide fractures are said to be about 5-25mm (DOE, 2004), a conservative estimate of 5mm for this study was assumed for all stages. For simplicity, a single planar fracture originating at the injection point was assumed to be representative of the effective fracture area.

We remark that only a subset of the detected microseismic events were processed by the contractor; therefore the fracture geometries determined are potentially underestimated since they are based on a subset of the microseismic data actually generated during the fracture treatment.

Radiated Seismic Energy

Lastly, the radiated seismic energy (ES) was calculated in order to determine how much of the energy output the actual microseismic events contributed. This is given in units of Joules by:

$$\log_{10}(E_S) = 1.5 M_0 + 4.8 \quad . \tag{4}$$

This equation is modified from Kanamori (1977), who used the Gutenberg-Richter magnitude-energy relation calibrated for large earthquakes and expressed the result in units of ergs. M0 denotes moment magnitude. Equation 4 was rearranged and the radiated seismic energy calculation was done for each microseismic event. Moment magnitudes for each individual event were provided by the contractor and are a measure of the microseismic source strength. Then, all of the energies were summed for each stage and a total seismic energy value was determined (Table 1).

Since only a subset of data was processed, not all of the microseismic events are represented in the above calculation. The implications of this are discussed in the next section.

Correction for missing data

The Gutenberg-Richter magnitude-recurrence relation is given by (Gutenberg and Richter, 1954):

$$\log_{10} N = a - bM_0 \quad , \tag{5}$$

where M is magnitude, N is the number of events greater than or equal to a given magnitude M0 and a and b are empirical parameters that are specific to a specific region or tectonic setting. This relation is widely used in earthquake seismology. The b value, in particular, is characteristic of the nature of seismicity.

Here we use observed microseismic data to estimate Gutenberg-Richter parameters for a fracture stage in order to assess the significance of missing data. These results are presented in Figure 1 and show, assuming that the reported events are complete for the top 4 magnitude bins, that the b value is approximately 1.7. Using these parameters along with the Kanamori relation for seismic energy, we estimated the number of events that are expected for this fracture stage to be between magnitude -3 and -0.5 as well as the associated energy. We found that the ratio of expected seismic energy to the energy in the subset of events reported by the contractor is 25.6.

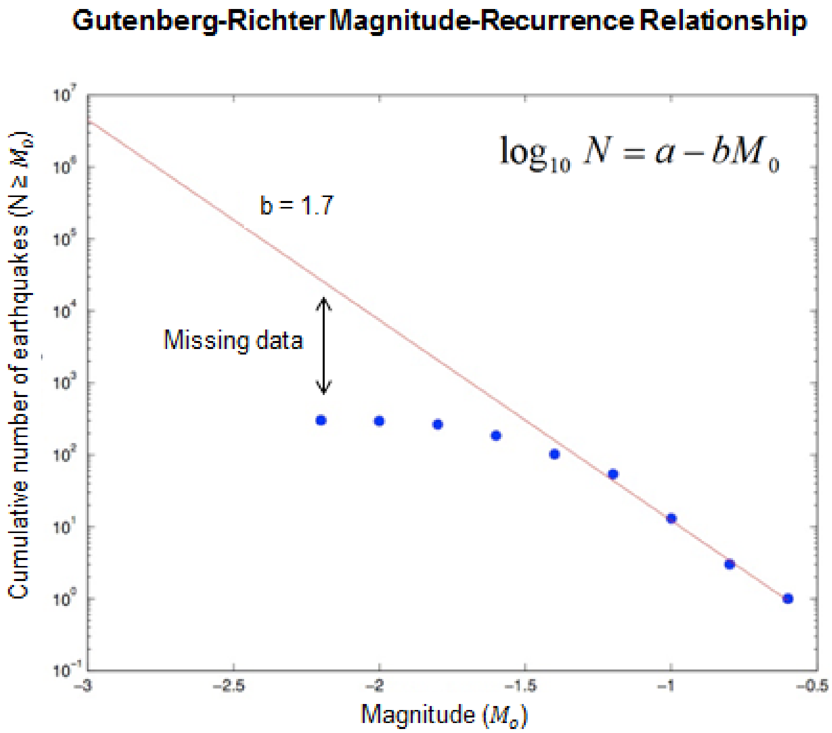

Figure 1 *Gutenberg-Richter plot for one fracture stage. Note missing data.*

This discrepancy between the expected energy and the seismic energy in the reported events is very significant. To our knowledge, this source of error has not been systematically considered in previous studies. We have applied a correction factor of 25.6 to all of our seismic energy estimates (Table 1).

Conclusions

Table 1 presents a summary comparing the various types of energy considered in this paper. It shows that between the fracture energy and the seismic energy, the fracture energy contributes the most to the total output energy. The injection energies for stage 1 on well #1 and stage 10 on well # 5 are higher than all of the other stages and this is because the fracture stimulations were the longest for these two stages.

Table 1. Summary and comparison of different energy values and their relationships

Well/Formation Name	Stage	Injection Energy (KJoules)	Fracture Energy (KJoules)	Seismic Energy (KJoules)	% Fracture Energy	% Seismic Energy
Well #1 (Otter Park)	Stage 1	192,647,400.00	29,168,562.50	9,996.79	15	0.03
	Stage 2	165,301,920.00	27,188,525.00	19,508.12	16	0.07
	Stage 3	154,350,000.00	22,137,500.00	4,641.58	14	0.02
Well # 2 (Otter Park)	Stage 4	163,838,400.00	40,035,000.00	9,230.97	24	0.02
Well # 3 (Muskwa)	Stage 5	140,829,120.00	34,979,600.00	28,055.40	25	0.08
	Stage 6	144,942,000.00	37,900,800.00	25,532.75	26	0.07
	Stage 7	162,035,040.00	66,409,750.00	32,141.91	41	0.05
	Stage 8	143,100,000.00	53,845,000.00	32,845.77	38	0.06
Well # 4 (Muskwa)	Stage 9	156,017,100.00	22,160,000.00	14,640.01	14	0.07
Well # 5 (Muskwa)	Stage 10	223,941,510.00	26,217,100.00	18,346.79	12	0.07

It was found that the fracture energy ranges from 12-41% of the total input energy. Some of the stages produced smaller percentages of fracture energy to injection energy ratios and overall, the fracture to energy ratios are on the low end of our prediction which stated that the fracture energy should be 20-80% of the total injection energy. The seismic energies for stage 1 and 2 on well #1 and stage 1 on well # 2 have the smallest seismic energy values partly either due to the number of events processed (i.e. fewer events processed then recorded) or the strength of the events (i.e. the magnitudes were relatively lower) for that stage. Stage 7 on well #3 had the largest percent of fracture energy to injection energy at 41%, this is primarily attributed to it having the largest fracture length.

Even after b-value corrections, the high-frequency seismic energy contribution still constitutes an infinitesimal part of the fracturing process, i.e. <1%. Though only a subset of data was available for this study, a more comprehensive understanding of the fracture geometry and microseismic magnitudes will help improve the estimates made in this paper. These improvements will mostly impact the fracture energy and radiated seismic energy calculations and provide better approximations of their percent contributions to the total deformation process.

Acknowledgements

The authors would like to thank Nexen Inc. for permission to use their data. We also benefited greatly from discussions with Norm Warpinski. The Sponsors of the Microseismic Industry Consortium are sincerely thanked for their support of this initiative.

References

Gutenberg B., and Richter, C.F. 1954. Seismicity of the Earth and Associated Phenomena, 2nd ed. Princeton, N.J.: Princeton University Press.

Hanks, T.C. and Kanamori, H., 1979. A moment magnitude scale. J. Geophysical Res., 84: 2348-2350.

Kanamori, H., 1977. The energy release in great earthquakes. AGU 7B0286: Vol. 82, No. 20.

Maxwell, S.C. Shemata, J. Campbell, E. and Quirk, D., 2008. Microseismic deformation rate monitoring. SPE 116596.

Pearson, C., 1981. The relationship between microseismicity and high pressures during hydraulic stimulations experiments in low permeability granitic rock. J. Geophysical Res. v. 86, p. 7855-7864.

Perkins, T.K., Kern, L. R., 1961. Widths of hydraulic fractures. SPE 89.

Warpinski, N.R., Wolhart, S.L. and Wright, C.A. 2004. Analysis and prediction of microseismicity induced by hydraulic fracturing. SPE 87673.

Department of Energy (DOE). 2004. Evaluation of impacts to underground sources of drinking water by hydraulic fracturing of coalbed reservoirs. Hydraulic Fracturing White Paper: http://www.epa.gov/ogwdw/uic/pdfs/cbmstudy_attach_uic_append_a_doe_whitepaper.pdf.